

# Tensegrity Structures for Mass-Efficient Planetary Landers

Edwin A. PERAZA HERNANDEZ, Raman GOYAL, Robert E. SKELTON\*

Department of Aerospace Engineering, Texas A&M University  
College Station, TX 77843

\* bobskelton@tamu.edu

## Abstract

In tensegrity, axially loaded 1-D members are methodically arranged to obtain an optimal structural response. These structures were inspired by Kenneth Snelson, who, as an artist, created topologies of this sort. The energy storage properties of a tensegrity topology known as the D-bar are determined analytically in this work. Such energy storage properties are compared against those of bent buckled beams, which have been proposed as components for mechanical energy absorption in planetary landers. An example comparing the energy storage capabilities of a tensegrity lander vehicle with D-bar structures against those of a vehicle with bent buckled beams is also presented. It is shown that D-bar structures of low complexity have higher energy storage and lower mass than bent beams; analogous results are determined in the example of the tensegrity lander. These results imply that D-bar structures can significantly enhance the response of planetary landers as well as other applications such as seismic-resistant buildings and micro-structured materials that would benefit from low-mass/high-energy absorption parts.

**Keywords:** tensegrity, energy absorption, compressive structures, self-similar iterations, planetary lander

## Tribute to Kenneth Snelson

*By Robert E. Skelton.* In 1992, I saw piece of art that changed my engineering career. I had designed control systems for spacecraft for many years, and learned that the structure and control design problems are not independent. On a vacation at the Kroller Muller Museum in the Netherlands in 1992 I stared at the Needle Tower for an hour, concluding that this artist had a better idea for structure design than any engineer I ever met. So I visited Kenneth Snelson in his Manhattan studio and marveled at his work ethic and ingenuity, and listened carefully to his frustration with engineers. City engineers in a certain country forced him to add a cable to support the end of his cantilevered tensegrity sculpture, since they had no mathematical proof that the structure would not fall on the sidewalk below. Snelson always had several scaled models of his designs to prove their structural integrity, but the engineers wanted math. Adding this extra cable to the art piece to please the engineers destroyed the artistic appeal of the piece and disappointed Snelson. Listening to Snelson tell this story reminded me that engineers often use elegant math to analyze uninspired structures, whereas artists build inspired structures without the math. I offered to Snelson free analysis of loads in his next project, if he wanted it, to show the benefit of engineer/artist collaborations. Even though Snelson never took advantage of this offer, this conversation caused me to abandon my previous approaches to structure and control design. It was obvious that tensegrity was the right paradigm to integrate the two disciplines. Today a new frontier in engineering emerges, involving universities around the world, seeking to make more efficient use of natural material resources to design structures for revolutionary new engineering capabilities, from bridges, to morphing aircraft wings, to structures swimming in the ocean, to fabrication of structures in space, all adopting the tensegrity paradigm inspired by Kenneth Snelson [1, 2, 3]. Biologists have shown that tensegrity is

the architecture of life, as each cell and each skeleton/muscle arrangement show. Thank you Kenneth Snelson for your inspirational impact on art, biology, and engineering. The engineers love you now. I hope you have forgiven them.

## 1 Introduction

Tensegrity allows for the development of structures with optimal properties or responses by methodically arranging networks of 1-D elements [4, 5]. These structures were inspired by the pioneer artist Kenneth Snelson, who created beautiful topologies of this sort. Buckminster Fuller gave them the name tensegrity. A *tensegrity system* is defined as a structurally stable network of axially loaded pre-stressable members [4]. These load-carrying members are classified as *strings* (subject to axial tensile loads) and *bars* (subject to axial compressive loads). Tensegrity structures of various topologies have been mathematically proven to optimally (i.e., with minimum mass) sustain compressive, bending, and torsional loads when compared to their continuum counterparts (e.g., a single beam or a torsional rod); see [4]. These structures will give engineers the material topologies they need to create optimal allocations of mass and stiffness, and allow the pioneering work by Snelson to develop a maturity in the engineering world and enable more efficient designs for robots, civil structures, and space structures.

The feasibility of a tensegrity topology known as the *D-bar* [4] for applications in mechanical energy absorption systems is explored here. As shown in Fig. 1(b), a D-bar structure of *complexity* 1 is obtained by replacing a compressive component with 6 rectilinear bars and 3 strings. A D-bar structure of complexity  $q$  is obtained by replacing each bar of a D-bar of complexity  $q - 1$  with a D-bar of complexity 1. It is known that D-bar structures support compressive loadings with minimal mass under buckling and material yielding constraints as compared to single columns [4]; however, their mechanical energy absorption properties have not been studied yet.

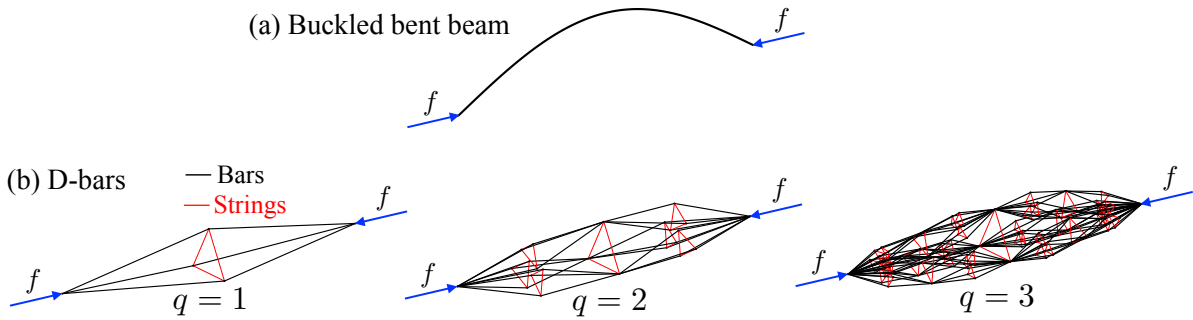


Figure 1: (a) A buckled bent beam subject to a compressive load  $f$ . (b) D-bar structures of different complexity  $q$  subject to a compressive load  $f$ .

Potential applications of D-bar structures as low-mass energy absorption components include space lander vehicles. SunSpiral and coworkers [6] designed tensegrity bots for planetary exploration that can safely absorb impact energy. Rimoli [7, 8] extended the approach of [6] to design a planetary lander with buckled beams that absorb the kinetic energy of the vehicle during landing. Here we investigate whether the mass and energy absorption capabilities of space lander vehicles can be enhanced by replacing their compressive members with D-bar structures. Other applications of D-bar tensegrity structures for mass-efficient mechanical energy storage include micro-structured metamaterials formed by tensegrity lattices [9] and buildings with enhanced seismic-resistance [10].

The objective of this study is to explore the *mechanical energy stored* in a D-bar structure subject to a compressive force (Fig. 1(b)) and compare it to that stored in a bent buckled beam under the same

boundary conditions (Fig. 1(a)). As previously stated, beams bent due to buckling have been recently proposed as energy absorption components in tensegrity landers [7] and therefore provide a comparison point. The analytical formulation of the energy stored in a D-bar structure is presented, and then the comparisons between the energy stored in the D-bar structure and a bent beam at the single component level and as parts of a tensegrity lander assembly are provided.

## 2 Energy Stored and Minimal Mass of a Bent Buckled Beam

This section provides analytical formulas for the *mechanical (elastic) energy stored* ( $V_B$ ) and the *minimal mass* ( $m_B$ ) of a bent buckled beam subject to an axial compressive force of magnitude  $f$ . The presented results are based on Euler-Bernoulli beam theory and Euler theory of buckling. Since the beam is subject to a single axial compressive load, it is assumed that the beam is in a post-buckled state. The beam has length  $l$  and is made of a homogeneous and isotropic material with Young's modulus  $E_b$ , yield stress  $\sigma_b$ , and mass density  $\rho_b$ . The beam has a uniform circular cross-section of radius  $r$ . In Euler theory of buckling, the critical buckling load  $f$  and the beam deflection  $w$  are given as:

$$f = \frac{\pi^3 E_b r^4}{4l^2}, \quad w = w_{max} \sin\left(\frac{\pi x}{l}\right), \quad (1)$$

where  $w_{max}$  is the maximum deflection of the beam and  $x \in [0, l]$ . To calculate the highest mechanical energy stored in the bent beam, it is assumed that the beam is loaded to the onset of failure. In the post-buckled state studied here, failure occurs when the stress at any point of the bent beam reaches the yield stress  $\sigma_b$ . The maximum allowable deflection of the beam  $w_{max}$  that occurs at the onset of material yield and the strain  $\varepsilon$  of the beam at such a maximum deflection are given as:

$$w_{max} = \frac{l^2 \sigma_b}{\pi^2 r E_b}, \quad \varepsilon = y \frac{\sigma_b}{r E_b} \sin\left(\frac{\pi x}{l}\right), \quad (2)$$

where  $y \in [-r, r]$ . The mechanical energy stored in the bent beam  $V_B$  at post-buckling is obtained by integrating the strain energy density  $\frac{1}{2} E_b \varepsilon^2$  over the entire volume of the beam:

$$V_B = \int_{vol} \frac{1}{2} E_b \varepsilon^2 dv = \frac{l^2 \sigma_b^2}{8} \left( \frac{f}{\pi E_b^3} \right)^{\frac{1}{2}}. \quad (3)$$

It can also be shown that the minimal mass of the beam  $m_B$  is given as [4]:

$$m_B = 2l^2 \rho_b \left( \frac{f}{\pi E_b^3} \right)^{\frac{1}{2}}. \quad (4)$$

## 3 Energy Stored and Minimal Mass of D-bar Tensegrity Structures

This section provides the analytical equations for the *mechanical (elastic) energy stored* ( $V_D$ ) and *minimal mass* ( $m_D$ ) of a D-bar structure subject to an axial compressive force of magnitude  $f$ . The strings and the bars of the D-bar structure are made of homogeneous, isotropic, linear elastic materials. The geometry of D-bar structures of complexity  $q = 1, 2$  is illustrated in Fig. 2. The total length of the D-bar structure is denoted by  $l$ . The angle between the line connecting the end points of each D-bar unit and the line along any of its associated bars is denoted by  $\alpha$ .

As shown in Fig. 2, the length of *all* the bars in a D-bar structure of complexity  $q$  is denoted by  $l_q$ . The number of bars in a D-bar structure is denoted by  $n_b$ . It can be verified that:

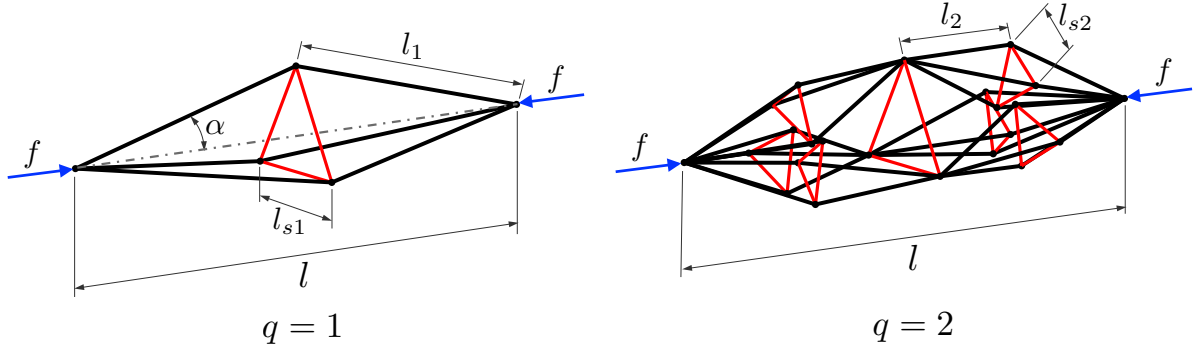


Figure 2: Geometric parameters of D-bar tensegrity structures of complexities  $q = 1$  and  $q = 2$ .

$$l_q = \frac{l}{(2 \cos(\alpha))^q}, \quad n_b = 6^q. \quad (5)$$

The length of the strings introduced in each increment of complexity is denoted by  $l_{si}$ ,  $i = 1, \dots, q$  and the number of such strings is denoted by  $n_{si}$ . It can also be verified that:

$$l_{si} = \frac{3^{\frac{1}{2}} l \tan(\alpha)}{2^{i-1} \cos^i(\alpha)}, \quad n_{si} = 2^{i-1} 3^i \quad i = 1, \dots, q, \quad (6)$$

The magnitude of the compressive force in *all* the bars of the D-bar structure, denoted by  $f_q$ , and the tensile force in the strings introduced in each complexity increment, denoted by  $t_i$ , are given as [4]:

$$f_q = \frac{f}{(3 \cos(\alpha))^q}, \quad t_i = \frac{2f \tan(\alpha)}{3^{i+\frac{1}{2}} \cos^{i-1}(\alpha)} \quad i = 1, \dots, q. \quad (7)$$

After studying the geometry and force distribution of D-bar structures with arbitrary complexity, the energy stored and minimal mass under material yield and buckling constraints are determined.

**Theorem 3.1.** Consider a D-bar structure of length  $l$ , complexity  $q$ , and angle parameter  $\alpha$  subject to a compressive force  $f$  applied at its end points. All the strings and bars are loaded up to the onset of failure corresponding to reaching the material yield stress in the strings and the critical buckling force in the bars. The material of the bars has Young's modulus  $E_b$  and mass density  $\rho_b$  and the material of the strings has Young's modulus  $E_s$ , mass density  $\rho_s$ , and yield stress  $\sigma_s$ . Then, the total mechanical energy stored in the D-bar structure  $V_D$  is given as:

$$V_D = \frac{2^{q-2}}{3^{\frac{q}{2}} \cos^{\frac{3q}{2}}(\alpha)} \left( \frac{\pi f^3}{E_b} \right)^{\frac{1}{2}} + \frac{l f \sigma_s (\sec^{2q}(\alpha) - 1)}{2 E_s}, \quad (8)$$

and its minimal mass  $m_D$  is given as:

$$m_D = \frac{3^{\frac{q}{2}} \rho_b l^2}{2^{q-1} \cos^{\frac{5q}{2}}(\alpha)} \left( \frac{f}{\pi E_b} \right)^{\frac{1}{2}} + \frac{l f \rho_s (\sec^{2q}(\alpha) - 1)}{\sigma_s}. \quad (9)$$

The formula for  $V_D$  is obtained by adding the contributions from the strain energy of all the strings and bars in the tensegrity structure when they are loaded to the onset of failure. Chapter 3 of [4] has a formula for mass  $m_D$  that includes additional strings that connect the end points of each D-bar unit. Such strings are not required in a minimal mass design for a D-bar.

#### 4 Comparison of Energy Stored and Mass of a D-bar Structure and a Bent Beam

##### 4.1 Single Component Assessment

To compare a D-bar structure with a bent beam, the ratio of energy stored in a D-bar to that of a bent beam ( $V_D/V_B$ ) and the ratio of the mass of a D-bar to that of a bent beam ( $m_D/m_B$ ) are calculated. The ratio  $V_D/V_B$  is obtained by dividing  $V_D$  from Eq. (8) by  $V_B$  from Eq. (3):

$$\frac{V_D}{V_B} = \frac{2^{q+1}}{3^{\frac{q}{2}} \cos^{\frac{3q}{2}}(\alpha)} \left( \frac{\pi E_b}{\sigma_b^2} \right) \left( \frac{f^{\frac{1}{2}}}{l} \right)^2 + \frac{4\sigma_s(\sec^{2q}(\alpha) - 1)(\pi E_b^3)^{\frac{1}{2}}}{E_s \sigma_b^2} \left( \frac{f^{\frac{1}{2}}}{l} \right). \quad (10)$$

Also, the ratio  $m_D/m_B$  is obtained by dividing  $m_D$  from Eq. (9) by  $m_B$  from Eq. (4):

$$\frac{m_D}{m_B} = \frac{3^{\frac{q}{2}}}{2^q \cos^{\frac{5q}{2}}(\alpha)} + \frac{\rho_s(\sec^{2q}(\alpha) - 1)(\pi E_b)^{\frac{1}{2}}}{2\sigma_s \rho_b} \left( \frac{f^{\frac{1}{2}}}{l} \right). \quad (11)$$

The length  $l$  and force  $f$  appear only in the parameter  $f^{\frac{1}{2}}/l$  in Eqs. (10)–(11). This parameter can be used as a scaling factor in the design of D-bars for energy storage across different scales. Contour plots for ratio of energy stored in a D-bar structure to a bent beam ( $V_D/V_B$ ) are shown in Fig. 3(a) for  $f^{\frac{1}{2}}/l = 100 \text{ N}^{\frac{1}{2}}/\text{m}$  and  $150 \text{ N}^{\frac{1}{2}}/\text{m}$ . Standard material parameters of aluminum are assumed for the beam, bars, and strings ( $E_b = E_s = 60 \text{ GPa}$ ,  $\sigma_b = \sigma_s = 110 \text{ MPa}$ ,  $\rho_b = \rho_s = 2700 \text{ kg/m}^3$ ). The axes of the contour plots correspond to the D-bar structure complexity  $q$  and angle  $\alpha$  (refer to Fig. 2). As indicated in Fig. 3(a), for different values of  $f^{\frac{1}{2}}/l$ , there exist D-bar structures of low complexity (between  $q > 1$  and  $q > 2$ ) that have higher energy stored than that of the bent beam (i.e., for which  $V_D/V_B > 1$ ).

Figure 3(b) shows contours of the ratio for the mass of the D-bar structure to the bent beam ( $m_D/m_B$ ). The regions where  $m_D/m_B < 1$  correspond to D-bar designs with lower mass than bent beams for the same value of  $f^{\frac{1}{2}}/l$ . There are D-bar structures of any complexity for which  $m_D/m_B < 1$  provided that  $\alpha$  is lower than  $\approx 17^\circ$ . Figure 3(c) shows the regions where D-bar structures are favorable by having lower mass and higher energy storage corresponding to the intersections of the regions where  $V_D/V_B > 1$  in Fig. 3(a) and  $m_D/m_B < 1$  in Fig. 3(b). Figure 3(c) shows that lower D-bar complexities have better performance than bent beams for higher values of  $f^{\frac{1}{2}}/l$  (i.e., higher values of compressive force  $f$  and lower values of length  $l$ ). Such trends indicate that D-bar structures are useful as mass-efficient energy absorption components in space systems subject to large impact forces and having limited volumes.

##### 4.2 Assembly-level Assessment

After comparing the energy stored and mass for single D-bar structures and bent beams, we now consider an example of a lander vehicle to further demonstrate the advantages of replacing beams that undergo buckling with D-bar structures for systems that take compressive loads. The example of the tensegrity planetary lander developed by SunSpiral and coworkers [6] is considered. The lander has 24 tensile members and 6 compressive members. To simulate impact conditions, vertical loads are applied on the top three nodes of the structure and the bottom three nodes are fixed as shown in Fig. 4(a). The total load applied to the top surface is denoted  $F$ . To determine the forces in each member of the lander, the equilibrium equations for tensegrity structures developed in [11] are employed.

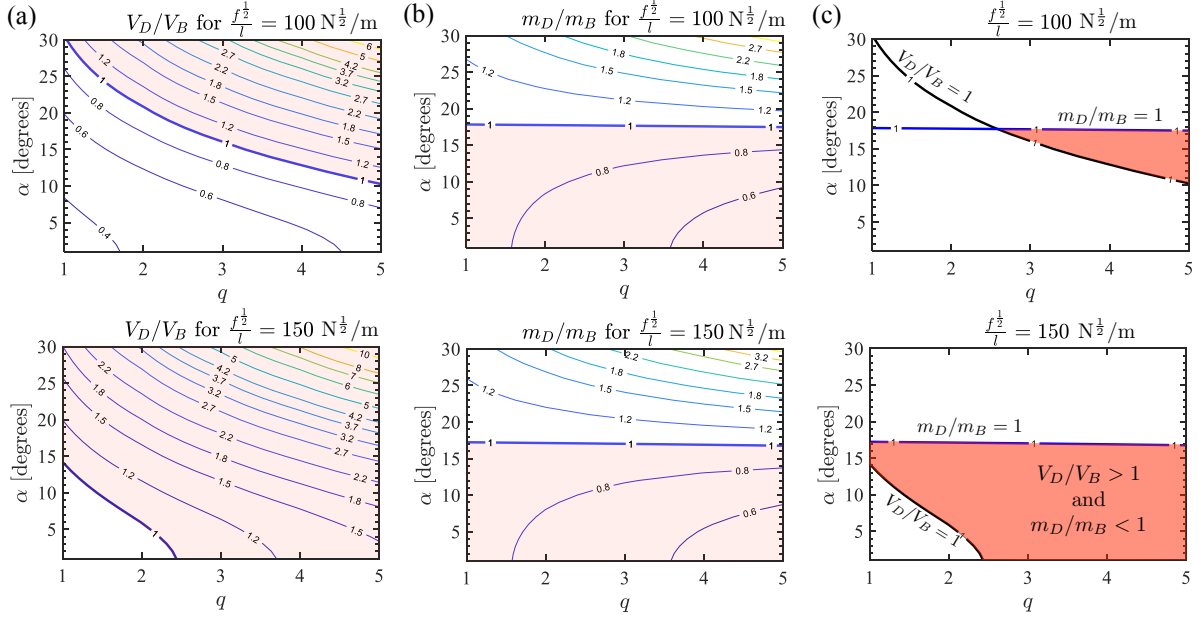


Figure 3: (a) Contours for ratio of mechanical energy stored for the D-bar to the bent beam ( $V_D/V_B$ ). (b) Contours for ratio of mass for the D-bar to the bent beam ( $m_D/m_B$ ). (c) Regions showing the design space of D-bar structures for which  $V_D/V_B > 1$  and  $m_D/m_B < 1$ .

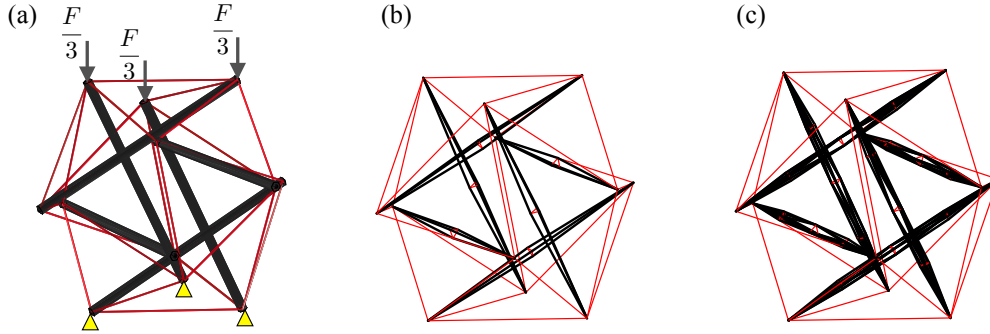


Figure 4: (a) Geometry and boundary conditions for a tensegrity lander [6]. The strings (red) have length  $\left(\frac{3}{8}\right)^{1/2} L$  and the beams (blue) have length  $L$ . The yellow triangles indicate the fixed nodes. (b) Tensegrity lander obtained by replacing the beams with D-bars of complexity  $q = 1$ . (c) Tensegrity lander obtained by replacing the beams with D-bars of complexity  $q = 2$ .

The strings take a tensile load  $t$  and are made of a material with Young's modulus  $E_s$ , yield stress  $\sigma_s$ , and mass density  $\rho_s$ . The compressive members take a load  $f$  of the lander are made of a material with Young's modulus  $E_b$ , and mass density  $\rho_b$ . In a minimum mass design, if the compressive members of the lander are beams that undergo buckling, its stored energy  $V_{SB}$  and mass  $m_{SB}$  are given as:

$$V_{SB} = 24 \left(\frac{3}{8}\right)^{1/2} \frac{\sigma_s L t}{2E_s} + (6) \frac{L^2 \sigma_b^2}{8} \left(\frac{f}{\pi E_b^3}\right)^{1/2}, \quad m_{SB} = 24 \left(\frac{3}{8}\right)^{1/2} \frac{\rho_s L t}{\sigma_s} + (6) 2L^2 \rho_b \left(\frac{f}{\pi E_b^3}\right)^{1/2}. \quad (12)$$

Conversely, if the compressive members of the lander are D-bar structures, its stored energy  $V_{SD}$  and

mass  $m_{SD}$  are given as:

$$V_{SD} = 24 \left( \frac{3}{8} \right)^{\frac{1}{2}} \frac{\sigma_s L t}{2 E_s} + 6 \left( \frac{2^{q-2}}{3^{\frac{q}{2}} \cos^{\frac{3q}{2}}(\alpha)} \left( \frac{\pi f^3}{E_b} \right)^{\frac{1}{2}} + \frac{L f \sigma_s (\sec^{2q}(\alpha) - 1)}{2 E_s} \right), \quad (13)$$

$$m_{SD} = 24 \left( \frac{3}{8} \right)^{\frac{1}{2}} \frac{\rho_s L t}{\sigma_s} + 6 \left( \frac{3^{\frac{q}{2}} \rho_b L^2}{2^{q-1} \cos^{\frac{5q}{2}}(\alpha)} \left( \frac{f}{\pi E_b} \right)^{\frac{1}{2}} + \frac{L f \rho_s (\sec^{2q}(\alpha) - 1)}{\sigma_s} \right). \quad (14)$$

The two designs are now compared. Again, standard material parameters of aluminum are assumed for the beams, bars, and strings ( $E_b = E_s = 60$  GPa,  $\sigma_b = \sigma_s = 110$  MPa,  $\rho_b = \rho_s = 2700$  kg/m<sup>3</sup>). Values of  $F = 15000$  N and  $L = 1$  m are assumed. These values resulted in  $f = 22360$  N and  $t = 9128$  N. Ratios of mechanical energy stored and mass for the two designs are shown in Fig. 5. In the  $m_{SD}/m_{SB}$  contour, it is observed that landers with D-bars have lower mass than landers with bent beams for the entire domain of complexities ( $q$ ) studied. The  $V_{SD}/V_{SB}$  contour shows that the lander with D-bars also has higher energy stored for all complexities. The design region for a lander with D-bar structures which stores more energy ( $V_{SD}/V_{SB} > 1$ ) and requires less mass ( $m_{SD}/m_{SB} < 1$ ) than a lander with bent buckled beams is also shown in Fig. 5. Overall, the results shown in Fig. 5 indicate that designs of tensegrity landers can be significantly enhanced if D-bar structures of low complexities are integrated.

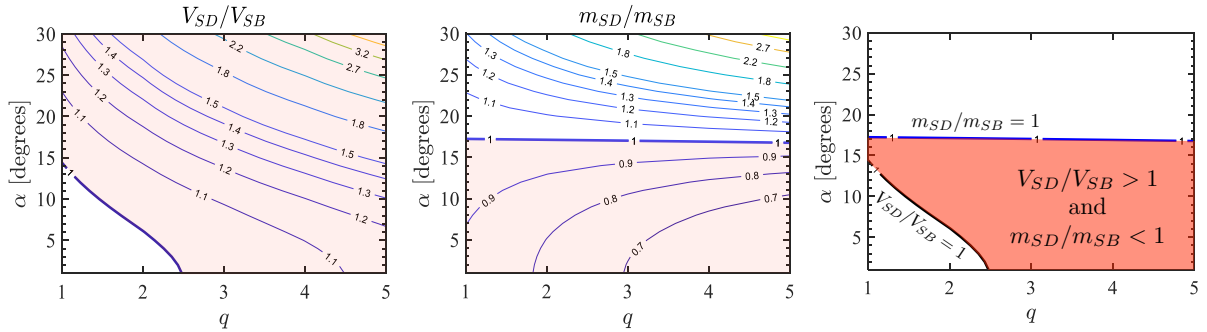


Figure 5: Contours for ratios of mechanical energy stored ( $V_{SD}/V_{SB}$ ), total mass ( $m_{SD}/m_{SB}$ ), and design region with  $V_{SD}/V_{SB} > 1$  and  $m_{SD}/m_{SB} < 1$  for tensegrity landers whose compressive members are D-bar structures or beams that undergo buckling. Standard material parameters of aluminum are assumed for the beams, bars, and strings.

## 5 Summary and Concluding Remarks

The feasibility of D-bar tensegrity structures as mass-efficient mechanical energy absorption components was examined. Analytical expressions were determined for the stored mechanical energy and minimal mass of D-bar structures and bent beams (recently proposed as components for mechanical energy absorption in bars/strings networks). The analytical expressions for stored mechanical energy in post-buckled beams and D-bar structures have not been presented before and are the key contributions of the present work.

Comparisons of the energy stored and minimal mass of bent buckled beams and those of D-bars were provided. For practical ranges of compressive force magnitude and beam/D-bar length, there exist D-bar systems of relatively low complexity that have higher energy storage and require less mass than the bent buckled beam. Lower D-bar complexities have better performance than bent beams for higher values of compressive force magnitude and lower values of beam/D-bar length. Such trends indicate that D-bar

structures can be useful as mass-efficient energy absorption components in space systems subject to high impact loads and placed in small volumes. The energy storage and minimal mass of tensegrity landers with D-bar structures or buckled beams as its compressive members were also compared. Replacing the bent buckled beams with D-bar structures resulted in more energy stored and less mass across the entire complexity range. The presented results imply that space vehicles can greatly benefit from D-bar structures as low-mass energy absorption components for use during landing and other maneuvers that involve vehicle impact.

## References

- [1] K. Snelson. Snelson on the tensegrity invention. *International Journal of Space Structures*, 11(1-2):43–48, 1996.
- [2] K. Snelson. The art of tensegrity. *International Journal of Space Structures*, 27(2-3):71–80, 2012.
- [3] K. Snelson. Continuous tension, discontinuous compression structures, February 16 1965. US Patent 3,169,611.
- [4] R. E. Skelton and M. C. de Oliveira. *Tensegrity Systems*. Springer, 2009.
- [5] R. Motro. Tensegrity systems: the state of the art. *International Journal of Space Structures*, 7(2):75–83, 1992.
- [6] V. SunSpiral, G. Gorospe, J. Bruce, A. Iscen, G. Korbel, S. Milam, A. Agogino, and D. Atkinson. Tensegrity based probes for planetary exploration: Entry, descent and landing (EDL) and surface mobility analysis. *International Journal of Planetary Probes*, 7, 2013.
- [7] J. J. Rimoli. A reduced-order model for the dynamic and post-buckling behavior of tensegrity structures. *Mechanics of Materials*, 116:146 – 157, 2018. IUTAM Symposium on Dynamic Instabilities in Solids.
- [8] J. J. Rimoli. On the impact tolerance of tensegrity-based planetary landers. In *57th AIAA/ASCE/AHS/ASC Structures, Structural Dynamics, and Materials Conference*, page 1511, 2016.
- [9] D. De Tommasi, G.C. Marano, G. Puglisi, and F. Trentadue. Morphological optimization of tensegrity-type metamaterials. *Composites Part B: Engineering*, 115:182 – 187, 2017. Composite lattices and multiscale innovative materials and structures.
- [10] A. Sadeghi and F. Seifollahi. Seismic behavior of tensegrity barrel vaults. In *Symposium of the International Association for Shell and Spatial Structures (50th. 2009. Valencia). Evolution and Trends in Design, Analysis and Construction of Shell and Spatial Structures*. Editorial Universitat Politècnica de València, 2009.
- [11] R. Goyal and R. E. Skelton. Dynamics of class 1 tensegrity systems including cable mass. In *16th Biennial ASCE International Conference on Engineering, Science, Construction and Operations in Challenging Environments*, 2018.